Parametric interaction of the electric and acoustic fields in a sapphire monocrystal transducer with a microwave readout

C. R. Locke,[a] M. E. Tobar, E. N. Ivanov, and D. G. Blair
Department of Physics, The University of Western Australia, Nedlands 6907, Western Australia, Australia

(Received 15 June 1998; accepted for publication 15 September 1998)

A sapphire monocrystal configured with a parametric microwave readout can potentially monitor the motion of its internal acoustic resonances at the precision governed by quantum mechanical fluctuations. The mechanism of transductance is due to parametric interaction between the electric and acoustic field within the crystal. This mechanism has been tested for the first time, and the theory has been verified by observing the pump frequency dependence of the acoustic quality factor. Because of the extremely low acoustic losses ($Q>10^7$) and electrical losses ($Q>10^4$), measurements were sensitive enough to attain positive verification at room temperature. © *1998 American Institute of Physics.* [S0021-8979(98)04024-9]

I. INTRODUCTION

Parametric interactions between mechanical and electrical waves in dielectric materials has been described previously.[1] Sapphire has an intrinsic advantage over other materials as a high quality transducer due to its low intrinsic acoustic and electromagnetic losses.[2] Due to the strain dependence of the dielectric mode frequencies in the sapphire monolith, the system has intrinsic electromechanical transducer properties. The sapphire bar dielectric transducer (SBDT) studied in this work is a monocrystal cylinder of ''HEMEX'' grade sapphire 100 mm long and 50 mm in diameter, manufactured by Crystal Systems Inc. with low levels of impurities. The SBDT operates as a parametric transducer, consisting of an external pump signal tuned to a dielectric resonance, which is then modulated by the acoustic oscillations of the sapphire bar. This can be thought of as a resonant inductor/capacitor/resistor (LCR) circuit coupled to a mass/spring system, in which the oscillating mass changes the capacitance of the LCR circuit. The main mechanism of this modulation is due to the strain dependence of the polarizability of the internal crystal electric field, which manifests as a strain dependent permittivity. To obtain the most sensitive operation, high order whispering gallery (WG) dielectric resonances are excited inside the SBDT. The energy of these modes is confined near the circumference of the cylindrical surface. These modes exhibit large electrical frequency-displacement tuning coefficients (df/dx) of order 10^{12} Hz/m, and high electrical quality factors of order 10^5 at room temperature. In this article the parametric interaction between the acoustic bar oscillations and a WG dielectric resonance is demonstrated by observing the acoustic losses as the pump frequency is varied, with theory agreeing very well with measurements.

It has been shown that when using an acoustic harmonic oscillator such as the SBDT as a detector, there is a sensitivity limit similar to the Heisenberg uncertainty principle due to the quantum mechanical nature of the observation and is known as the standard quantum limit (SQL). Cryogenic techniques which exploit the ultralow mechanical and electrical losses of sapphire at low temperatures are necessary to attain quantum limited sensitivity. Explicitly, it has been shown that state-of-the-art pump oscillator technology and cooling to 4 K is required,[3] as is an improved suspension system[4] to reduce seismic noise. No measurement of a classical force or variable has been made *below* the SQL, in which the mechanical oscillator detecting the classical force is coupled to another oscillator which is the transducer readout system. The readout is set sensitive to only one quadrature with all the uncertainty driven into the other quadrature; this process is known as squeezing and for a quantum system is called quantum nondemolition (QND). To date researchers have only developed the classical analogue known as back action evasion (classical squeezing).

Results presented in this article have verified the operation principles of the SBDT. We believe further continuation of this work will see the SBDT achieving for the first time measurements of the SQL, and then by applying the principles of squeezing this could also lead to the first acoustic QND measurement. For a detailed assessment of achieving this possibility, see Ref. 3.

A. Mechanism of transductance

The fundamental longitudinal acoustic resonance of the SBDT under investigation is close to 50 kHz. As the acoustic oscillator resonates, the dimension of the crystal changes and strain is induced within the crystal. Thus, two main mechanisms of transductance exist: (a) due to the alteration of the crystal dimension as it oscillates, and (b) due to the strain induced change in permittivity. Figure 1 shows exaggerated changes in the dimensions of the oscillating SBDT.

To calculate the dielectric resonant frequency in a sapphire cylinder, a proven separation of variables technique has been used.[5] This leads to a transcendental equation of the following form which can be solved numerically:

$$F(f,\varepsilon_{\parallel},\varepsilon_{\perp},x,r)=0. \tag{1}$$

Here f is the electromagnetic resonant frequency, $\varepsilon_{\parallel}$ is the permittivity parallel to the crystal c axis, and $\varepsilon_{\perp}$ is the per-

[a]Electronic mail: clocke@pd.uwa.edu.au

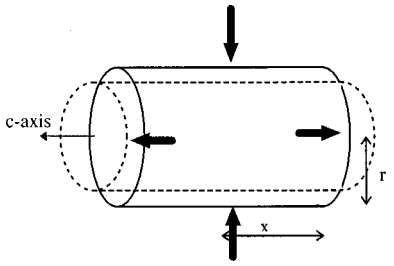

FIG. 1. Change in shape of the SBDT oscillating in a longitudinal mode with respect to the half length, x, and radius, r. The change in half length is related to the change in radius by Poisson's ratio. The crystal c axis is aligned with the cylindrical z axis for symmetry and to obtain good mechanical and electrical Q values.

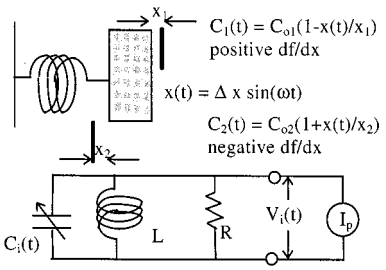

FIG. 2. Capacity transducer model for the sapphire bar dielectric transducer (SBDT). The pump source is modelled by an effective current source at the pump frequency, while the output is represented by the induced voltage $V_i(t)$ across the equivalent resonant LCR circuit. The fundamental acoustic resonance is modeled as a mass spring element of effective mass of half the bar mass. The motion modulates the effective capacitance due to the change in shape and the strain induced change of permittivity in the crystal. This in turn modulates the transducer electrical resonant frequency. Positive tuning coefficients are represented by $C_1(t)$, while negative tuning coefficients are represented by $C_2(t)$, which shows the displacement modulation acting 180° out of phase with respect to a positive tuning coefficient.

mittivity perpendicular to the crystal c axis. For sapphire, the anisotropic components of permittivity are known very accurately[6,7] and the dimensions are easily measured. Thus, Eq. (1) may be solved to predict accurately the resonant frequencies. To calculate the expected transductance (df/dx) the induced change in the variables $\varepsilon_{\parallel}$, $\varepsilon_{\perp}$ and r must be known with respect to a change in x. The perturbed electromagnetic resonant frequency, $f+\Delta f$, due to a displacement Δx can thus be calculated from

$$F\left(f+\Delta f, \varepsilon_{\parallel}+\frac{d\varepsilon_{\parallel}}{dx}\Delta x, \varepsilon_{\perp}+\frac{d\varepsilon_{\perp}}{dr}\frac{dr}{dx}\Delta x, x+\Delta x, r+\frac{dr}{dx}\Delta x\right)=0. \tag{2}$$

As long as the value of Δx is sufficiently small with respect to x, and sufficiently large not to be dominated by numerical errors, an accurate prediction of the transductance may be calculated by comparing Eqs. (1) and (2) to calculate df/dx. For sapphire, Poisson's ratio is approximately 0.3 and thus the relation between x and r is $\Delta r/r \approx -0.3\Delta x/x$. Thus, $dr/dx \approx -0.15$ for the aspect ratio of the SBDT under investigation.

B. Capacity transducer model of the parametric effects

Parametric effects are intrinsic to systems where a mechanical resonance is coupled to an ac pumped electrical circuit. These effects are observable in low loss systems, where electromagnetic coupling and electrical and mechanical quality factors are large.[8] Without loss of generality, it is possible to model parametric effects using a capacitance modulation scheme, where a resonant mechanical motion modulates the capacitance of an effective LCR circuit excited near resonance by an ac pump signal. Depending on the phase relation between the mechanical oscillator and pump oscillator, a parametric force acts on the acoustically oscillating mass. The force acts to change the quality factor and resonant frequency of the acoustic resonance by providing additional damping and by adding to the spring constant, respectively.

Models for positive tuning coefficient transducers have been derived previously.[9–11] The SBDT transducer has the property that the TM modes in the crystal have negative tuning coefficients with respect to displacement. This stems from the monolithic nature of the transducer and the mechanism of the tuning coefficient as described previously. All other dielectric or cavity transducers that modulate a gap spacing have positive tuning coefficients for all TM and TE modes.[8–12] Thus, it has been necessary for us to generalize previous models to allow a negative tuning coefficient to describe the parametric effects observed in the SBDT. A capacity transducer model which highlights the difference between transducer modes with positive and negative tuning coefficients is shown in Fig. 2.

Assuming that the modulation creates sidebands at only $\pm\omega$ (the acoustic modulation frequency), from the pump frequency, Ω_p, we can write the output voltage, $V_i(t)$ (where subscript $i=1$ or 2 refer to transducers with positive and negative tuning coefficients, respectively):

$$V_i(t)=V_{oi}[\cos(\Omega_p t)+a_{i+}\cos(\Omega_+ t)+b_{i+}\sin(\Omega_+ t)+a_{i-}\cos(\Omega_- t)+b_{i-}\sin(\Omega_- t)]. \tag{3}$$

Here V_{oi} is the amplitude of the output voltage at the pump frequency, $\Omega_{\pm}=\Omega_p\pm\omega$, $a_{i\pm}$ are the in phase modulation coefficients at $\Omega_{\pm}$, and $b_{i\pm}$ are the quadrature modulation coefficients at $\Omega_{\pm}$.

To calculate the parametric effects, the force on the antenna due to the electric field across the capacitor must be calculated. For both positive and negative tuning coefficient capacitor models this may be easily shown to be[9]

$$F_i(t)=\frac{C_{oi}}{2x_{oi}}V_i(t)^2. \tag{4}$$

By substituting Eqs. (3) into (4) and by ignoring any frequency terms higher than ω (these terms are in practice negligible), it follows that

$$F_i(t)=\frac{C_{oi}}{4x_{oi}}V_{oi}^2+\frac{C_{oi}}{2x_{oi}}V_{oi}^2[(a_{i+}+a_{i-})\cos(\omega t)+(b_{i+}-b_{i-})\sin(\omega t)]=F_{DC\,i}+F_{M\,i}(\omega t). \tag{5}$$

The first term is a dc term which exists in the absence of the modulation, which we expect to be the same for both positive and negative tuning coefficient models. However, since the modulation is 180° out of phase between models, we may expect the modulation coefficients to have opposite sign. We proceed to show that this is indeed true.

To calculate the modulation coefficients, we assume the output voltage, V_i, is of the form given by Eq. (3) and we sum the currents in R_i, L_i, and C_i and equate them to the pump current. The pump current represents the incident signal and is void of any modulation sidebands and is thus given by

$$I_p(t) = I_A \cos(\Omega_p t) + I_B \sin(\Omega_p t). \tag{6}$$

The currents through the capacitor, inductor, and resistor are respectively given by

$$I_{C_i}(t) = C_i \frac{dV_i}{dt} + V_i \frac{dC_i}{dt}; \quad I_{L_i}(t) = \frac{\int V_i dt}{L_i}; \quad I_{R_i}(t) = \frac{V_i}{R_i}. \tag{7}$$

From the substitution of Eq. (5) into (7), the in-phase ($\cos[\Omega_{\pm} t]$) and quadrature ($\sin[\Omega_{\pm} t]$) components at frequencies $\Omega_{\pm}$ can be collected to give

$$\begin{aligned} a_{1\pm} &= -a_{2\pm} = \pm \frac{\Delta x Q_{ei} \Omega_{\pm}}{2 x_{oi} \Omega_{oi}} \frac{1}{(4Q_{ei}^2 \Delta_{i\pm}^2 + 1)}; \\ b_{1\pm} &= -b_{2\pm} = \pm \frac{\Delta x Q_{ei} \Omega_{\pm}}{2 x_{oi} \Omega_{oi}} \frac{2Q_{ei} \Delta_{i\pm}}{(4Q_{ei}^2 \Delta_{i\pm}^2 + 1)}. \end{aligned} \tag{8}$$

Here, Q_{ei} and Ω_{oi} are the electrical quality factor and resonant frequency of the equivalent LCR circuits, $\Delta_{i\pm} = ((\Omega_p - \Omega_{oi}) \pm \omega)/\Omega_{oi}$, and $i = 1$ or 2.

By substituting Eq. (8) into Eq. (5), the input impedance [Ns/m] seen by the acoustic oscillator at frequency ω, may be calculated by isolating the term $F_{M\,i}(\omega t)/(\omega \Delta x)$. It is conventional to write this impedance as a complex phasor, where $F_{M\,i}(\omega t)/(\omega \Delta x) = \mathrm{Re}[Z_i e^{j\omega t}]$. For a positive tuning transducer ($i = 1$) and using $\Omega_{\pm}/\Omega_{oi} = 1 + \Delta_{i\pm}$, the complex input impedance Z_1 may be calculated to be

$$\mathrm{Re}[Z_i] = \frac{C_{oi} V_{oi}^2 Q_{ei}}{4.\omega.x_{oi}^2} \left(\frac{1 + \Delta_{i+}}{4Q_{ei}^2 \Delta_{i+}^2 + 1} - \frac{1 + \Delta_{i-}}{4Q_{ei}^2 \Delta_{i-}^2 + 1} \right), \quad i = 1, \tag{9a}$$

$$\begin{aligned} \mathrm{Im}[Z_i] = &- \frac{C_{oi} V_{oi}^2 Q_{ei}}{4.\omega.x_{oi}^2} \\ &\times \left[\frac{2Q_{ei} \Delta_{i+} (1 + \Delta_{i+})}{4Q_{ei}^2 \Delta_{i+}^2 + 1} \right. \\ &\left. + \frac{2Q_{ei} \Delta_{i-} (1 + \Delta_{i-})}{4Q_{ei}^2 \Delta_i^2 + 1} \right], \quad i = 1, \end{aligned} \tag{9b}$$

and for the negative tuning coefficient case, the input impedance Z_2 is calculated to be $-Z_1$. Thus, the input impedance when $i = 2$ is 180° out of phase compared to the case when $i = 1$. Because we are studying a microwave system, it facilitates our comparison of experiment with theory if we can write the input impedance in terms of microwave parameters rather than the equivalent LCR circuit parameters. This is done by substituting the following relations[11] into Eq. (9):

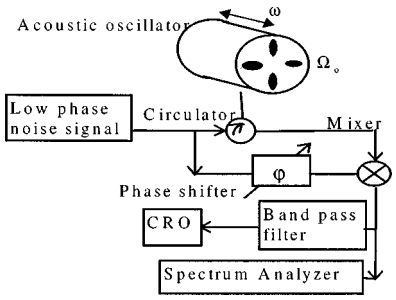

FIG. 3. Microwave readout used to measure the acoustic Q factor and mechanical frequency (ω) using the high Q dielectric whispering gallery modes (Ω_0) at 10 GHz.

$$\begin{aligned} C_{oi} V_{oi}^2 &= \frac{8 Q_{ei} P_{\mathrm{inc}}}{\Omega_{oi}} \frac{\beta_{ei}}{(1 + \beta_{ei})} \frac{1}{(1 + 4Q_{ei}^2 \Delta_i^2)}; \\ \frac{1}{4x_{oi}^2} &= \frac{1}{f_{oi}^2} \left(\frac{df}{dx} \right)_i^2, \end{aligned} \tag{10}$$

where P_{inc} is the incident power, Q_{ei} becomes the loaded electrical Q, β_{ei} the electrical coupling, and Δ_i the detuning from the electrical resonance $(\Omega_p - \Omega_{oi})/\Omega_{oi}$.

It has been shown that the modified acoustical resonant frequency and quality factor can be written as[10,13]

$$\omega_{\mathrm{Li}} = \omega \sqrt{1 - \frac{\mathrm{Im}[Z_i]}{m\omega}}, \quad Q_{\mathrm{Li}}^{-1} = Q^{-1} + \frac{\mathrm{Re}[Z_i]}{m\omega}. \tag{11}$$

Equations (9a) and (9b) show the real and imaginary part of the mechanical impedance vary as a function of the system parameters. Their magnitudes scale as $V^2 Q$ which demonstrates that their effects will only be large for high incident power and high electric Q factor systems. The changes in the real part of the impedance ($\mathrm{Re}[Z]$) correspond the changes in the acoustic losses of the system; the microwave interaction can cause the net acoustic loss of the system to vary. The imaginary part of the impedance ($\mathrm{Im}[Z]$) corresponds to variations in the stiffness of the mechanical system, corresponding to changes in the mechanical resonant frequency [see Eq. (11)]. Calculations were performed using these equations to determine the magnitude of parametric effects at room temperature in the SBDT. To see how the calculated and measured calculations compare see Sec. III.

II. EXPERIMENTAL SETUP

A parametric transducer, as shown in Fig. 3, was set up to measure the mechanical resonant frequency and ring-down time (or mechanical quality factor) of the SBDT. A low phase noise pump oscillator signal was coupled to the $\mathrm{TM}_{14\,1\,1}$ WG mode at 10 GHz (transverse magnetic with 14 nodes around the radius, 1 down the length of the bar, and 1 node radially). The mechanical resonance adds sidebands to the reflected signal at $\pm\omega$ offset from the microwave carrier. The signal was then mixed with a phase shifted portion of carrier signal which was adjusted such that the system was phase sensitive (standard phase bridge read out).

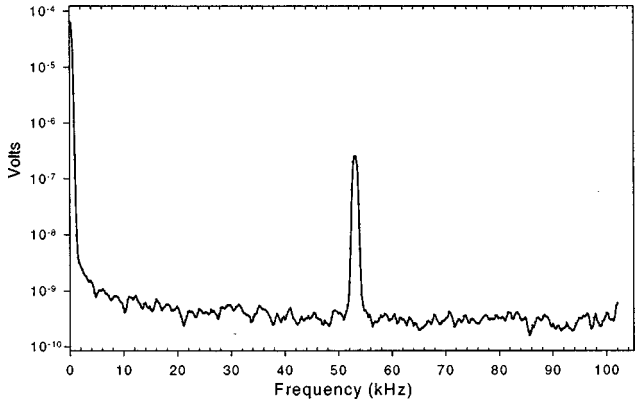

FIG. 4. Frequency spectrum of SBDT when mechanically excited in its longitudinal acoustic resonance.

The resonant frequency and quality factor were then measured by mechanically exciting the sapphire and observing the frequency spectrum and time evolution of the sidebands added to the carrier frequency. A bandpass filter was used to eliminate any harmonic distortion. The resonant frequency was measured to be 53.04 kHz on the spectrum analyzer (see Fig. 4), while the Q factor was measured to be 2.3×10^7 from the time evolution captured on a digital CRO (see Fig. 5). The measured resonant frequency was verified as the fundamental longitudinal resonance of the sapphire cylinder from finite element modeling, which predicted a frequency of 54.3 kHz. Measurements were done in vacuum at a pressure below 0.05 Torr.

The above results were obtained with the microwave pump oscillator tuned to the dielectric TM resonance. As the frequency of the pump oscillator is adjusted, parametric effects cause the acoustic frequency and quality factor of the SBDT to change. These effects were measured and were compared to the theory introduced in Sec. I. Results are reported in the following section.

III. COMPARISON OF EXPERIMENT AND THEORY

Parametric effects were observed using the setup described previously. High microwave input power of order 1 W was used to enhance these effects. Experimental parameters during the measurement process were; $m=0.4$ kg (half the bar mass), $\omega/(2\pi)=53.3$ kHz, $Q_m=2.3\times10^7$, $Q_e=6.0\times10^4$, $\beta_e=0.52$, $df/dx=-1.26\times10^{12}$ Hz/m, $P_{\text{inc}}=1.10$ W, $f_0=10.03$ GHz.

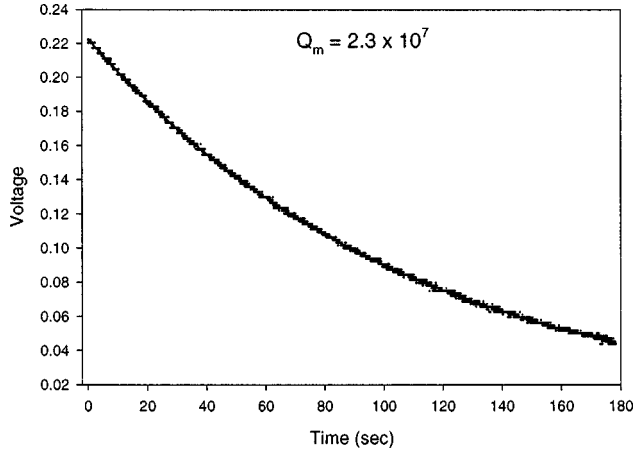

FIG. 5. Experimentally observed ringdown curve of the acoustic resonance.

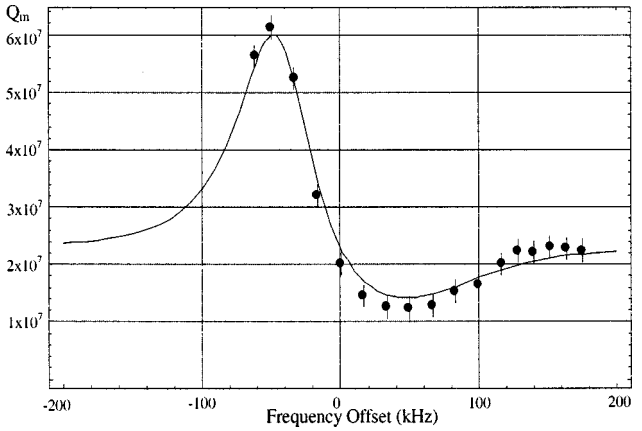

FIG. 6. Mechanical quality factor versus pump frequency offset from the $TM_{14\,1\,1}$ resonance, clearly showing parametric effects. Solid curve is the theoretical curve obtained from Eq. (11) and the experimentally measured parameters as given in Sec. III. The plotted points are the measured values calculated from the ring down curves captured on the CRO. Error estimation is shown by error bars.

As the microwave pump frequency was swept across the resonant frequency, changes in the mechanical ringdown times were observed and then compared against theoretical predictions. Figure 6 shows a comparison of theory derived using Eq. (11) versus experimentally measured mechanical quality factors. Below the pump oscillator resonance, the phase of the microwave signal acts to excite the mechanical resonance, enhancing the quality factor (parametric regeneration). Above resonance, the phase of the microwave signal acts to damp the acoustic oscillations, reducing the quality factor (cold damping). From the quality factor versus pump oscillator frequency characteristic shown in Fig. 6, it is clear from the comparison of theory and experiment we are observing a parametric effect. This result can be contrasted with a gap spaced modulated reentrant cavity or sapphire transducer, which has a positive tuning coefficient (df/dx), resulting in cold damping below resonance and active excitation above.

Although sapphire is anisotropic, it has been assumed in this derivation that $d\epsilon/dx$ is isotropic, and $d\varepsilon_{\parallel}/dx=d\varepsilon_{\perp}/dr$. There is some discrepancy in the literature regarding change in permittivity due to strain; for the purposes of our calculations the relationship $d\varepsilon/\varepsilon\approx14(dx/x)$ was used, which is an average of values given in literature.[2,14] This experiment does not yield sufficient information to determine an accurate value for this parameter. However, current work involves the construction of a cryogenic experiment that will enable accurate determination of change in permittivity due to strain.

IV. CONCLUSION

We have experimentally verified the interaction between the electric and acoustic fields in a sapphire monocrystal by monitoring the acoustic losses. The experimental results

agree closely with theory. Due to the negative tuning coefficient of the SBDT, the parametric interaction leads to cold damping for the pump frequency above resonance, opposite to the effect observed in conventional parametric systems. If these results are extrapolated to cryogenic temperatures where mechanical quality factor is expected to be $\sim 10^{10}$ and electrical quality factors may be 10^9, and the parametric interaction will dominate the dynamics of the sapphire resonator. Accurate measurements of this interaction will yield accurate data on the dependence of permittivity due to strain in sapphire. By separately selecting TM and TE modes, anisotropic effects may also be measured. Future work will investigate a high sensitivity cryogenic version of this experiment.

ACKNOWLEDGMENTS

The authors thank Ju Li and Mitsuru Taniwaki for the help on the suspension system that was needed to make quality factor measurements. This work was funded by the Australian Research Council.

[1] I. L Bajak, Wave Electron. **8**, 51 (1977).
[2] V. B. Braginsky, V. P. Mitrofanov, and V. I. Panov, *Systems with Small Dissipation* (Chicago University Press, Chicago, 1985).
[3] M. E. Tobar, E. N. Ivanov, D. K. L. Oi, B. D. Cuthbertson, and D. G. Blair, Appl. Phys. B: Lasers Opt. **64**, 153 (1997).
[4] M. Taniwaki, L. Ju, D. G. Blair, and M. E. Tobar, Phys. Lett. A **246**, 37 (1998).
[5] M. E. Tobar and A. G. Mann, IEEE Trans. Microwave Theory Tech. **39**, 2077 (1991).
[6] R. Shelby and J. Fontanella, J. Phys. Chem. Solids **41**, 69 (1980).
[7] J. Krupka, K. Derzakowski, A. Abramowicz, M. Tobar, and R. G. Geyer, IEEE Trans. Microwave MTT (to be published).
[8] B. D. Cuthbertson, M. E. Tobar, E. N. Ivanov, and D. G. Blair, Rev. Sci. Instrum. **67**, 2435 (1996).
[9] R. P. Giffard and H. J. Paik, ''Derivation of relations between mechanical and electrical amplitudes for modulated resonator transducers,'' 1977.
[10] P. J. Veitch, in *The Detection of Gravitational Waves*, edited by D. G. Blair (Cambridge University Press, Cambridge, 1991), pp. 186–225.
[11] M. E. Tobar and D. G. Blair, J. Phys. D **26**, 2276 (1993).
[12] H. Peng, Ph.D. thesis, The University of Western Australia, 1995.
[13] V. B. Braginsky and F. Y. Khalili, *Quantum Measurement* (Cambridge University Press, Cambridge, 1992).
[14] A. N. Luiten, Doctor of Philosophy thesis, University of Western Australia, 1995.